Original Article

Ecological vulnerability assessment of the Ya'an-Qamdo section along the southern route of the Sichuan-Tibet transportation corridor

BAO Fang[1,2] (iD) https://orcid.org/0000-0003-2492-0031; e-mail: 190519720@qq.com

QIU Jian[1*] (iD) https://orcid.org/0000-0003-1382-0211; ✉ e-mail: qiujian@home.swjtu.edu.cn

Corresponding author

1 School of Architecture, Southwest Jiaotong University, Chengdu 611756, China

2 China Railway Eryuan Engineering Group Co., Ltd., Chengdu 610031, China

Abstract: Identifying the ecological vulnerability of the sensitive and fragile ecosystem of the Ya'an-Qamdo section along the southern route of the Sichuan-Tibet transport corridor is of paramount importance to reduce environmental damage resulting from infrastructure construction. This paper divided the Ya'an-Qamdo transport section into 22 subzones according to their ecological environment characteristics. Based on the vulnerability evaluation model established by the fuzzy matter-element analysis method, the eight main assessment indicators of ecological vulnerability were windstorm, rainstorm, snowstorm, extreme temperature, extreme air pressure, geological hazard, natural conditions, and social resources. The rating and ranking of vulnerability in each subzone were based on the weight of the judgment indicators. Scientific processes were used to verify the rationality of both the indicators themselves and their weights. The results of this study show that subzone 9, located in the subalpine cold and humid forest and scrubland zone, is the most vulnerable, and subzone 1, located in the low- to mid-land warm and humid forest zone, is the least vulnerable. The conclusion of the study suggests that targeted measures of ecological protection should be formulated before development and construction of major transportation infrastructure. Construction should evade the most vulnerable areas, and in-depth research on ecological restoration should be carried out in low- to mid-vulnerability areas so that the ecological environment along the route can be protected effectively for sustainable economic and social development.

Keywords: Ecosystem; Vulnerability; Subzone; Sichuan-Tibet transportation corridor

1 Introduction

Since the Qing Dynasty, the Sichuan-Tibet transportation corridor has been comprised of the northern "commercial route" and the southern "official route" (Qiao 2013). Both routes start from Ya'an, Sichuan and pass through Tianquan, Luding, and Kangding (originally Dajianlu). The northern route goes northwest to Ganzi and Derge, then west through Qamdo into Lhasa, Tibet. The southern route runs westbound through Litang, Batang, and Nyingchi into Lhasa. The beautiful and long-established Sichuan-Tibet transport corridor has rich and diverse ecosystems and natural landscapes, including forests, bushlands, meadows, and wetlands

(Ni et al. 2013; Luo et al. 2005). Many towns such as Ganzi and Dege on the northern route, and Litang and Batang on the southern route, are important economic and cultural centers of the region. As a typical region with Han and Tibetan cultures, it is important to build and develop the region reasonably so that its glorious natural beauty and unique culture can be showcased to the world. However, with diverse geological and harsh climatic conditions, the Sichuan-Tibet transport corridor is one of the most ecologically vulnerable areas worldwide. Due to global warming, increasing human activity, decreasing overall recovery capacity of the natural ecosystem, and a seriously threatened biodiversity, the region has presented the features of extreme sensitivity and extreme vulnerability (Li et al. 2003; Luo et al. 2004; Lai 1996).

Ecological vulnerability refers to the sensitivity and ecological resilience of an ecosystem to external disturbances under specific regional conditions and is the result of the internal succession of ecosystems and the interaction between natural factors and human activity (Wei et al. 2015). For an ecological vulnerability assessment, indicators are usually assigned to build measurable models for evaluation both at home and abroad, including the 'pressure-state-response' (PSR) model (Men and Liu 2018), the 'vulnerability scoping diagram' (VSD) model (Polsky et al. 2007; Li, Fan 2014; Chen et al. 2018), and the 'spatially explicit resilient vulnerability' (SERV) model (Frazier et al. 2014), with VSD being the most widely used. Established research involves a variety of quantitative assessment methods, which fall into two main categories: a) data assessment methods based on sampling (or historical data). This category is represented by principal component analysis (Abson et al. 2012; Kan et al. 2018), the TOPSIS method (Song et al. 2016; Yang et al. 2018), and the data envelopment method (Huang et al. 2019; Zhang and Liu 2013); b) methods for related problem-solving in uncertain environments under the domain of fuzzy mathematics. This category is mainly based on three theories: fuzzy mathematical theory, mutation theory, and matter-element extension theory (Zhang et al. 2009; Wang et al. 2019; Forootan, 2022). The main methods for determining the weights of judgment indicators are expert scoring, hierarchical analysis, entropy weighting, and evidence weighting (Chen et al. 2022; Li et al. 2011; Zou et al. 2021; Dagnino et al. 2008; Xia et al. 2016; Suter et al. 2020).

The Ya'an-Qamdo section has a complex topographic and geomorphological environment, which has attracted great attention from scholars for its ecological vulnerability. Literature review shows that existing studies have focused on sensitivity to external natural disturbances such as climate change, climatic hazards, and geological hazards (Zou et al. 2013; Gao et al. 2016; Guo 2017; Ma et al. 2019; Zhong et al. 2010; Zhang et al. 2004; Wang et al. 2021), which has laid a foundation for understanding the ecological context and environmental conditions along the route. However, with rapid economic and social development, the impact of human activity has become increasingly prominent. Existing research results have been unable to meet the practical needs of engineering and construction. Moreover, as the Sichuan-Tibet railway line has been announced to pass through this section, revealing its ecological vulnerability based on the impact of human activity and proposing quantitative evaluation methods will provide scientific and technological support for ecological environmental protection and sustainable economic and social development of the region along the line.

2   Study Area

In this paper, based on the scope of environmental assessment defined by the railway project construction (Jie et al. 2015), we identify the 10 km range on both sides of the centerline of the newly built railway line from Ya'an to Qamdo as the specific study object (Fig. 1). The main landscape formations of this section are the Sichuan Basin, the Hengduan Mountains, and the Qinghai-Tibet Plateau (Xu 1991). The Hengduan Mountain Range, which runs north-south in parallel rows, includes Qionglai Mountain, the Dadu River, Snowy Mountain, the Yalong River, Shaluli Mountain, the Jinsha River, Mangkang Mountain, the Lancang River, Nu Mountain, the Nujiang River, and Gaoligong Mountain. It is a vast and treacherous terrain with deep river valleys and fluctuations in elevation of up to 1,000-2,500 m, as well as diverse climate conditions including subtropical, plateau marine, and continental. With an altitude of more than 2,500 meters above sea level, the regions have remarkable climatic characteristics such as large daily fluctuations in temperature, uneven precipitation distribution,

Fig. 1 Diagram of study area (route position referring to Song et al. 2016)

Low- to mid-land warm and humid forest zone

Subalpine river valley arid scrubland and grassland zone

Subalpine cold and humid forest and scrubland zone

Alpine hill and high plain river valley arid scrubland and grassland zone

Alpine hill and high plain scrubland and grassland zone

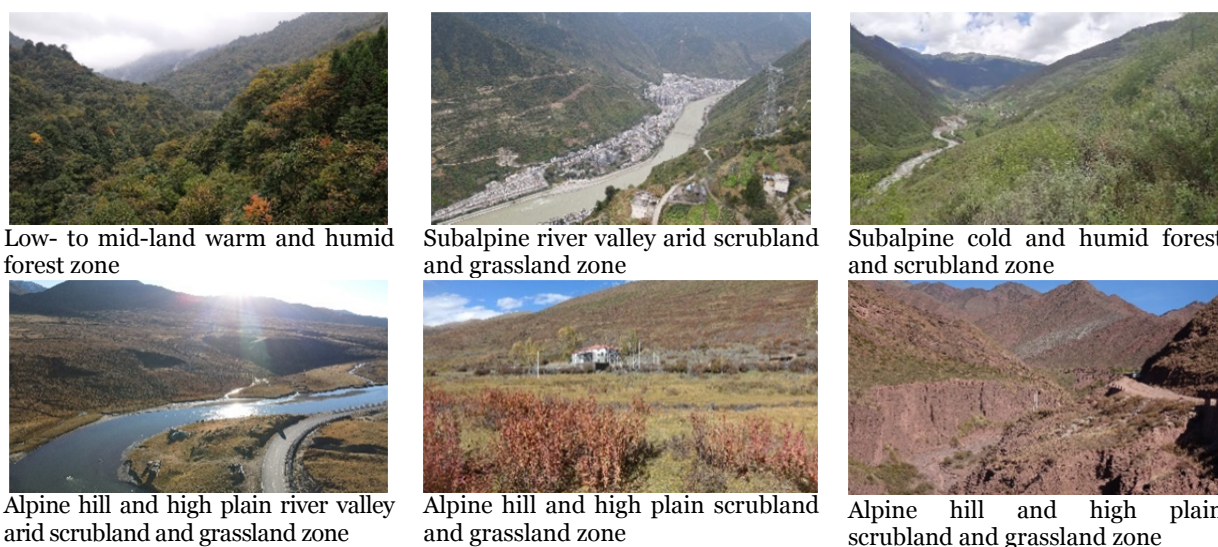Alpine hill and high plain scrubland and grassland zone

Fig. 2 Typical ecological zones on the Ya'an-Qamdo section along the southern route of the Sichuan-Tibet transportation corridor.

and seasonal frosts. The river valleys are arid and have prominent hydrothermal conflicts, with annual evaporation reaching 3-6 times the amount of rainfall.

The geography of this section includes lowland, midland, subalpine, and alpine elevation levels, as well as river valleys. The corresponding climatic environment and ecosystem of each elevation level is complex and variable, including warm and humid forests, cold and humid forests, dry scrublands, and alpine meadows. Satellite film and GIS raster data were combined and used to assess ecological vulnerability more accurately. The section is divided into 22 ecological subzones falling under five categories: low- to mid-land warm and humid forest zone; subalpine cold and humid forest and scrubland zone; subalpine river valley arid scrubland and grassland zone; alpine hill and high plain scrubland and grassland zone; and alpine hill and high plain river valley arid scrubland and grassland zone (Fig. 2 and Fig. 3).

3 Methodology

3.1 Evaluation model

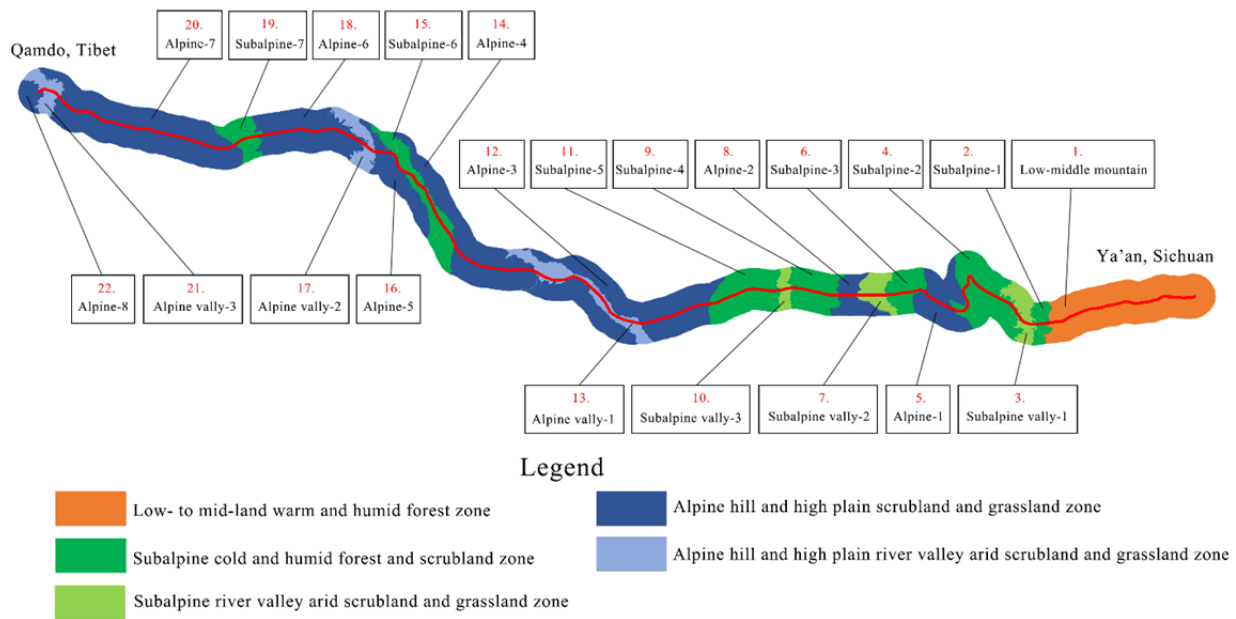A theoretical model for evaluating ecological

Fig. 3 Diagram of 22 ecological subzones on the Ya'an-Qamdo section along the southern route of the Sichuan-Tibet transportation corridor.

vulnerability was constructed based on previous research results and the fuzzy matter-element analysis method (Bao and Qiu 2021). The model summarizes 20 influencing factors of ecological vulnerability, including temperature, precipitation, snowfall, herbaceous cover, number of plant species, population density, and GDP per capita. Under the VSD vulnerability analysis framework, the 20 influencing factors are generalized into eight judgment indicators, and an indicator evaluation system is established accordingly.

In addition, Python programming software was used to construct a multi-factor and multi-attribute ecological vulnerability assessment and measurement model by combining fuzzy mathematics and physical element analysis (Xu et al. 2021). After obtaining the base scores of each judgment indicator through cluster analysis and determining each one's weight based on fuzzy matter-element analysis, we finally ranked the comprehensive vulnerability scores of each subzone. Among them, the judgment indicator base score $\varphi_i = \sum_{j=1}^{k} p_j \cdot s_j$ (φ_i denotes the i th judgment indicator score, s_j denotes the rank score of the partitioned judgment indicators contained in class $j(j=1,2,\ldots,k)$, and p_j denotes the weight of the rank score of class $j(j=1,2,\ldots,k)$); create object element $R = \left(x_{ji}\right)_{n \times m}$ (x_{ji} denotes the j th base score of judgment indicator in the i th scheme M_i, m

represents the number of schemes, n represents the number of assessment indicators), and pre-process the data based on the object element to obtain the compound fuzzy matter elements: $L = \left(\xi_{ji}\right)_{n \times m}$ (ξ_{ji} as the correlation coefficient), and calculate correlation compound fuzzy matter elements based on compound fuzzy matter elements $R_k = R_w \cdot L = \min\left(1, \sum_{j=1}^{n} R_{wj}\xi_{jk}\right)$, where

$$R_w = \left[\frac{\sum_{i=1}^{m}\xi_{1i}}{\sum_{j=1}^{n}\sum_{i=1}^{m}\xi_{ji}}, \frac{\sum_{i=1}^{m}\xi_{2i}}{\sum_{j=1}^{n}\sum_{i=1}^{m}\xi_{ji}}, \cdots, \frac{\sum_{i=1}^{m}\xi_{ni}}{\sum_{j=1}^{n}\sum_{i=1}^{m}\xi_{ji}}\right]$$ is

the weighted sum of the k th element of the vector of decision indicator weights R_k for the k th column of L with a weight of R_w. Finally, the correlation values are ranked to obtain the ranking results P of each scheme.

This paper conducts an empirical study of a theoretical model of ecological vulnerability assessment by calculating, scoring, and ranking the vulnerability of 22 ecological subzones of the Ya'an-Qamdo section along the southern route of the Sichuan-Tibet transport corridor.

3.2 Data collection and analysis

Mathematical calculation began with data collection and analysis of specific indicators for each

of the 22 ecological subzones. Field sample research was used for the judgment indicators of herbaceous cover and number of plant species. A combination of field research and aerial photogrammetry was used for the judgment indicator of geological hazards, and GIS, remote sensing technology, and various statistical methods were used for data analysis. Specifically, we processed a large amount of data regarding meteorological stations and geological conditions such as elevation, slope rate, and slope direction.

3.3 Validation of the evaluation model

After calculating the scores and ranking, we investigated a validation method to address two problems that are rarely mentioned in existing research regarding the theoretical framework of subjective analysis, the rationality of the judgment indicators, and the validity of their weight assignments.

3.3.1 Rationality of judgment indicators

In order to verify the rationality of the judgment indicator scores, this paper proposes a new idea of partition clustering: Firstly, cluster analysis is done on 20 influencing factors (tertiary indicators) in each of the 22 subzones, with the number of clusters being $k_1 = 10$, so that all factors can be taken into full consideration and subzones with similar vulnerabilities can be clustered in the same class; then the 8 judgment indicator scores are calculated as k_1 clustering centers; finally, the k_1 are clustered according to the scores of the judgment indicators (secondary indicators), and the number of clusters is k_2, so the clustering results of each subzone are obtained as: $A(a_1, a_2, \cdots, a_{22})$, $a_i \in \{1, 2, \cdots, k_2\}$. For the 8 judgment indicator scores of 22 subzones calculated with the above method, a cluster analysis is performed, and the number of clusters is k_2, so the clustering result is $B(b_1, b_2, \cdots, b_{22})$, $b_i \in \{1, 2, \cdots, k_2\}$. If the indicator scores are rational, the clustering results $A(a_1, a_2, \cdots, a_{22})$ and $B(b_1, b_2, \cdots, b_{22})$ should be quite similar. In order to measure the similarity of clustering results $A(a_1, a_2, \cdots, a_{22})$ and $B(b_1, b_2, \cdots, b_{22})$, this paper puts forward the concepts of classification degree, aggregation degree, and

separation degree, see Definitions 2-4. If clustering results A and B are exactly the same, the clustering degree g reaches the maximum $g' = \max g$, and the separation degree reaches the maximum $d' = \max d$. Based on the aggregation degree and separation degree, this paper proposes a qualitative indicator η to measure the clustering similarity:

$$\eta = \frac{g \cdot d}{g' \cdot d'} \tag{1}$$

where $\eta \in (0, 1)$, the expression for η shows that its physical meaning is the degree of similarity between the clusters of A and B. The closer η is to 1, the more similar the clusters of A and B are, and the more rational the scoring model is.

Definition 1 (classification matrix): Define the classification matrix as K, where k_{ij} denotes the number of class i data in A and the number of class j data in B, and the matrix is expressed as:

$$K = \begin{bmatrix} k_{11} & k_{12} & \cdots & k_{1n} \\ k_{21} & k_{22} & \cdots & k_{2n} \\ \vdots & \vdots & \vdots & \vdots \\ k_{m1} & k_{m2} & \cdots & k_{mn} \end{bmatrix}$$

where the number of rows and columns of matrix K are the number of classifications of A and the number of classifications of B, respectively.

Example 1: Suppose the two clustering results are: $A(1, 1, 1, 2, 2, 3)$ and $B(2, 2, 3, 1, 1, 1)$, then the classification matrix $K = \begin{bmatrix} 0 & 2 & 1 \\ 2 & 0 & 0 \\ 1 & 0 & 0 \end{bmatrix}$

Definition 2 (Aggregation degree g): Define aggregation as the F-parametric number of the classification matrix K. The more similar the clustering results, the larger the number of paradigms and the greater the aggregation degree.

Definition 3 (Separation degree d): For the classification matrix K, only the largest element of each row is retained and the remaining elements become 0 to form a new matrix K'. The rank of the new matrix K' is calculated and defined as the degree of separation.

The physical meaning of separation degree: Select the largest j_k th cluster in B as the corresponding cluster of the i th cluster in A. The higher the degree of separation, the lower the probability that each cluster in A will have the same

corresponding cluster in B. A larger separation means that A and B are more similar. When A and B are exactly the same, K and K' is a diagonal matrix and the separation degree is at its maximum.

In summary, from the perspective of the physical meaning of aggregation degree and separation degree, if clustering results A and B are the same, then the aggregation and separation degrees reach the maximum; the greater the degrees of aggregation and separation, the more similar the clustering results of A and B are.

3.3.2 Validity of indicator weights

In order to verify whether the indicator weights are valid, the eight indicators of the 22 subzones are subjected to cluster analysis. The vulnerability scores and vulnerability ranking of the five clustering centers can be obtained based on the weights calculated by the fuzzy matter-element analysis method. The same method is applied again in each class to obtain the ranking of each subzone, thereby the vulnerability ranking vector Q of each subzone can be obtained. Then compare the similarity between Q and the vulnerability sorting result P obtained by the above algorithm. To illustrate the similarity of the sorting vectors obtained by the two methods, this paper calculates the cosine of the vector angle. Suppose the vector α is $(x_1, y_1)^T$, vector β is $(x_2, y_2)^T$, and the angle of α and β is θ.

Then the similarity of α and β can be expressed by the cosine value of θ, which is calculated as:

$$cos\theta = \frac{\alpha \cdot \beta}{|\alpha||\beta|} \qquad (2)$$

where $\cos\theta \in (0,1)$, the closer $\cos\theta$ is to 1, the smaller the angle between α and β, and the more similar α and β are.

In summary, the similarity of the two ranking results can be obtained by calculating the cosine of the vector angle for the two vectors Q and P. The rationality of the indicator weights can then be verified.

4 Results of Ecological Vulnerability Assessment

4.1 Judgment indicator scores

In this paper, based on the influencing factors of eight judgment indicators, including windstorm, rainstorm, snowstorm, extreme temperature, extreme air pressure, geological hazard, natural conditions, and social resources, the 22 subzones are clustered into three classes according to k=3, which are shown in Fig. 4. Taking windstorm as an example, its influencing factors include annual maximum wind speed and annual average wind speed. Data for both factors are clustered into three classes according to k=3, which are shown in Fig. 3(A), where subzones 1, 2, 3, 19, 20, 21, and 22, subzones 6, 10, 11, 12, 13, 14, 15, 16, 17, and 18, and subzones 4, 5, 7, 8, and 9 form the three classes.

According to the clustering results of Fig. 4, the rating of natural hazards in the 22 subzones can be determined. The subzone with the highest hazard rating has a score of s_1=1; the subzone with the second-highest hazard rating has a score of s_2=0.667; and the subzone with the lowest hazard rating has a score of s_3=0.333. Taking windstorm as an example, the blue subzone has the highest hazard rating, with a score of s_1=1; the yellow subzone has the second-highest hazard rating, with a score of s_2=0.667; and the green subzone has the lowest hazard rating, with a score of s_3=0.333. The score of each judgment indicator can be further determined for each of the 22 subzones. The results are shown in Table 1.

To illustrate the eight judgment indicators in each of the 22 subzones more accurately, a visual aid is created of the numerical results of Table 1 for mapping thermodynamic diagrams. The darker the color, the more vulnerable the subzone is to that particular hazard. Taking the windstorm hazard as an example, you can see clearly that subzone 8 is the most vulnerable, and subzones 21 and 22 are the least vulnerable (Fig. 5).

4.2 Weighting of judgment indicators

The data of the eight judgment indicators are brought into the weight calculation model. Among the eight indicators, windstorm, rainstorm, snowstorm, extreme temperature, extreme air pressure, geological hazard, and sensitivity are of the smaller the better type, and adaptability is of the larger the better type. The correlation coefficient values corresponding to each indicator in each of the 22 subzones can be obtained, and thus the compound fuzzy matter elements are:

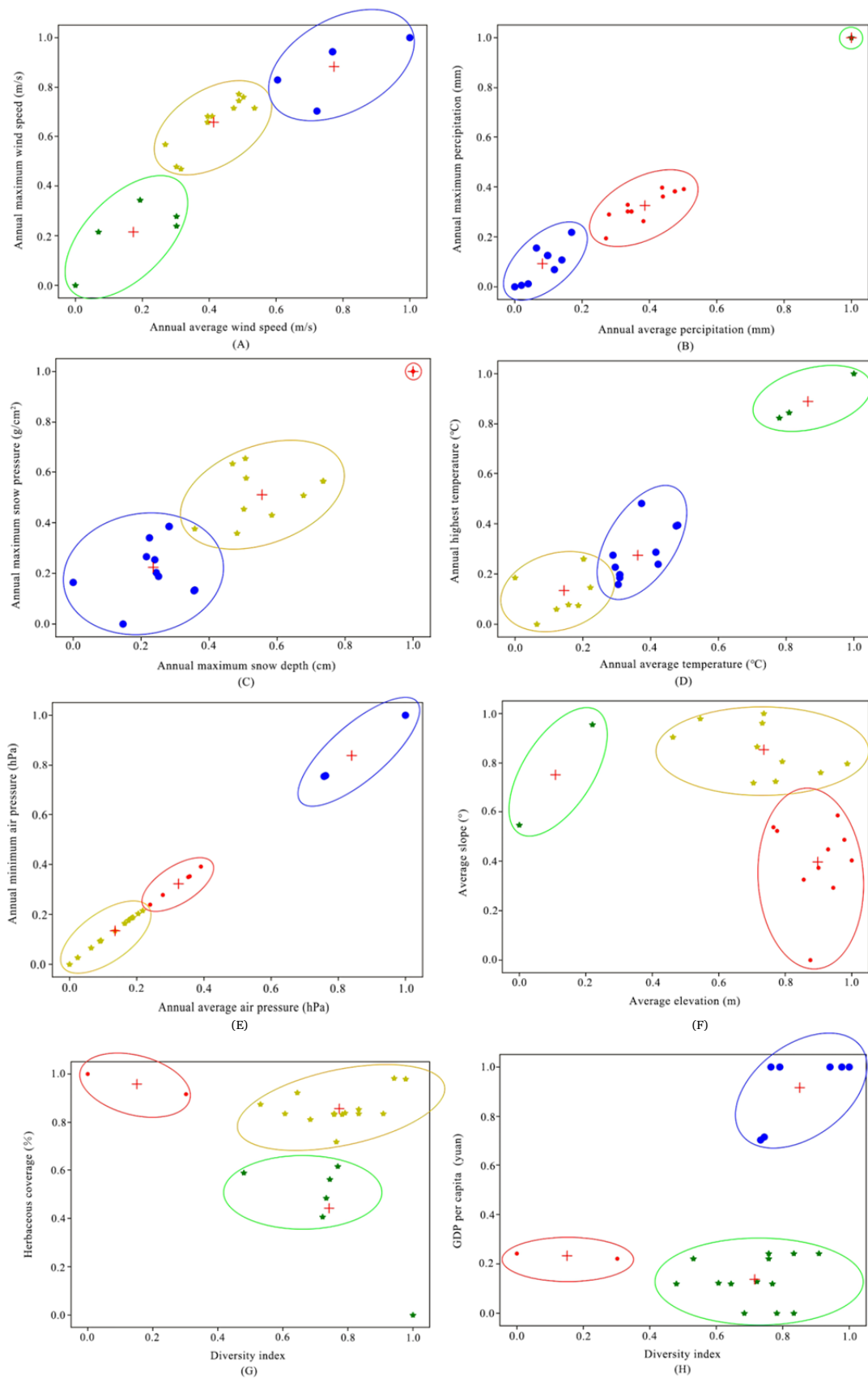$$L = \begin{bmatrix} L_{11} & L_{12} \\ L_{21} & L_{22} \end{bmatrix}$$

Fig. 4 Cluster analysis chart for the eight ecological vulnerability judgment indicators of the Ya'an-Qamdo section along the southern route of the Sichuan-Tibet transport corridor.

Table 1 Scoring summary of eight ecological vulnerability judgement indicators

No.	Scores						Sensitivity	Adaptability
	Exposure						Natural conditions	Social resources
	Windstorm	Rainstorm	Snowstorm	Extreme temperature	Extreme air pressure	Geological hazard		
1	0.56137	0.77931	0.54572	0.56442	0.52822	0.64563	0.79931	0.73416
2	0.54415	0.59944	0.52515	0.55613	0.51654	0.72119	0.78550	0.73665
3	0.54323	0.52659	0.52499	0.55528	0.51631	0.68731	0.81088	0.58626
4	0.79210	0.61602	0.78888	0.74999	0.74048	0.74615	0.75884	0.74795
5	0.77941	0.54998	0.78888	0.79109	0.81386	0.69808	0.82297	0.74660
6	0.69779	0.53868	0.52632	0.69124	0.76718	0.70711	0.76120	0.74810
7	0.80089	0.59338	0.69329	0.81670	0.82208	0.70966	0.76321	0.74729
8	0. 80089	0.59338	0.69329	0.81670	0.82208	0.68760	0.75025	0.74850
9	0.80116	0.57510	0.57819	0.80771	0.82124	0.74976	0.76043	0.56936
10	0.70433	0.53876	0.52606	0.69446	0.76977	0.73247	0.82952	0.54654
11	0.77028	0.53660	0.53837	0.81106	0.82198	0.74238	0.77420	0.59545
12	0.74710	0.54064	0.56375	0.82097	0.81941	0.68006	0.75033	0.58998
13	0.76123	0.52701	0.60876	0.81758	0.80983	0.65921	0.75541	0.57277
14	0.76805	0.51343	0.63713	0.81498	0.80287	0.69311	0.75141	0.59884
15	0.59608	0.51519	0.52273	0.75023	0.81835	0.74795	0.75036	0.60828
16	0.68707	0.51378	0.52307	0.79928	0.82174	0.73353	0.78339	0.55996
17	0. 68707	0.51378	0.52307	0.79928	0.82174	0.74362	0.83418	0.55093
18	0.76894	0.51287	0.61249	0.81055	0.79866	0.71683	0.85276	0.57932
19	0.56969	0.51399	0.52130	0.79701	0.82231	0.67962	0.76668	0.56251
20	0.57040	0.51872	0.53116	0.81768	0.81410	0.70321	0.75602	0.64391
21	0.54432	0.52142	0.53684	0.74444	0.80897	0.74068	0.75032	0.61266
22	0.53826	0.52002	0.52333	0.80158	0.82231	0.73820	0.75160	0.62954

of which:

$$L_{11} = \begin{bmatrix} 0.09 & 0.02 & 0.02 & 0.96 & 0.92 & 0.61 & 0.99 & 0.99 & 1 & 0.63 & 0.88 \\ 1 & 0.32 & 0.05 & 0.39 & 0.14 & 0.1 & 0.3 & 0.3 & 0.23 & 0.1 & 0.09 \\ 0.09 & 0.01 & 0.01 & 0.49 & 1 & 0.02 & 0.64 & 0.64 & 0.21 & 0.02 & 0.06 \\ 0.03 & 0.003 & 0 & 0.73 & 0.89 & 0.51 & 0.98 & 0.98 & 0.95 & 0.52 & 0.96 \end{bmatrix}$$

$$L_{21} = \begin{bmatrix} 0.04 & 0 & 0 & 0.73 & 0.97 & 0.82 & 0.99 & 0.99 & 0.99 & 0.83 & 0.99 \\ 0 & 0.72 & 0.40 & 0.96 & 0.50 & 0.59 & 0.61 & 0.40 & 1 & 0.83 & 0.93 \\ 0.48 & 0.34 & 0.59 & 0.08 & 0.71 & 0.11 & 0.13 & 0 & 0.1 & 0.77 & 0.23 \\ 0.07 & 0.06 & 0.80 & 0 & 0 & 0 & 0 & 0 & 0.89 & 1 & 0.76 \end{bmatrix}$$

$$L_{12} = \begin{bmatrix} 0.79 & 0.85 & 0.87 & 0.22 & 0.57 & 0.57 & 0.88 & 0.12 & 0.12 & 0.02 & 0 \\ 0.1 & 0.05 & 0 & 0 & 0 & 0 & 0 & 0 & 0.02 & 0.03 & 0.03 \\ 0.16 & 0.33 & 0.43 & 0 & 0 & 0 & 0.34 & 0 & 0.04 & 0.06 & 0.007 \\ 1 & 0.99 & 0.98 & 0.73 & 0.92 & 0.92 & 0.96 & 0.91 & 0.99 & 0.71 & 0.93 \end{bmatrix}$$

$$L_{22} = \begin{bmatrix} 0.99 & 0.96 & 0.94 & 0.98 & 0.99 & 0.99 & 0.92 & 1 & 0.97 & 0.96 & 1 \\ 0.33 & 0.13 & 0.46 & 0.98 & 0.84 & 0.94 & 0.68 & 0.33 & 0.55 & 0.91 & 0.89 \\ 0 & 0.05 & 0.01 & 0 & 0.32 & 0.82 & 1 & 0.16 & 0.06 & 0 & 0.01 \\ 0.78 & 0.87 & 0.74 & 0.69 & 0.93 & 0.98 & 0.84 & 0.92 & 0.52 & 0.67 & 0.59 \end{bmatrix}$$

From the equation for R_w, we have:

$$R_w = [0.14, 0.04, 0.05, 0.19, 0.21, 0.16, 0.07, 0.14]$$

Then the values of R_w and S are substituted by the correlation formula $R_k = R_w \cdot L$, thus obtaining

$$R_k = [R_{k1}, R_{k2}]$$

$$R_{k1} = [0.11, 0.17, 0.22, 0.63, 0.69, 0.46, 0.69, 0.65, 0.84, 0.69, 0.79]$$

$$R_{k2} = [0.68, 0.67, 0.71, 0.63, 0.75, 0.81, 0.81, 0.59, 0.58, 0.58, 0.61]$$

The vulnerability of each of the 22 subzones was rated by the degree of their correlation, and the results were

$\rho_1 < \rho_2 < \rho_3 < \rho_6 < \rho_{20} < \rho_{21} < \rho_{19} < \rho_{22} < \rho_4 < \rho_{15} < \rho_8 < \rho_{13} < \rho_{12} < \rho_5 < \rho_7 < \rho_{10} < \rho_{14} < \rho_{16} < \rho_{11} < \rho_{17} < \rho_{18} < \rho_9$

where ρ_i indicates the vulnerability of ith subzone. It can be seen that the most vulnerable is subzone 9, and the least vulnerable is subzone 1. The vulnerability rating of each of the 22 subzones is shown in Fig. 6.

5 Validation of Vulnerability Assessment Results

According to formulas 1 and 2 in section 3.3, we carried out rationality verification of the judgment indicators and the indicator weights in the ecological vulnerability assessment of the Ya'an-Qamdo section along the southern route of the Sichuan-Tibet transportation corridor. The results were as follows.

5.1 Validation of indicator scores

Taking $k_2=5$, a cluster analysis was performed for the eight indicator scores of the 22 subzones, and the results for subzone clustering A are:

(2 1 1 5 5 2 5 5 4 4 4 4 4 3 4 4 4 3 3 3 3)

According to the new subzone clustering idea, the results for subzone clustering B are:

(2 1 1 5 5 3 5 5 4 4 4 4 4 4 4 4 4 4 4 4 4)

(A) Windstorm

(B) Rainstorm

(C) Snowstorm

(D) Extreme temperature

(E) Exteme air pressure

(F) Geological hazard

(G) Natural conditions

(H) Social resources

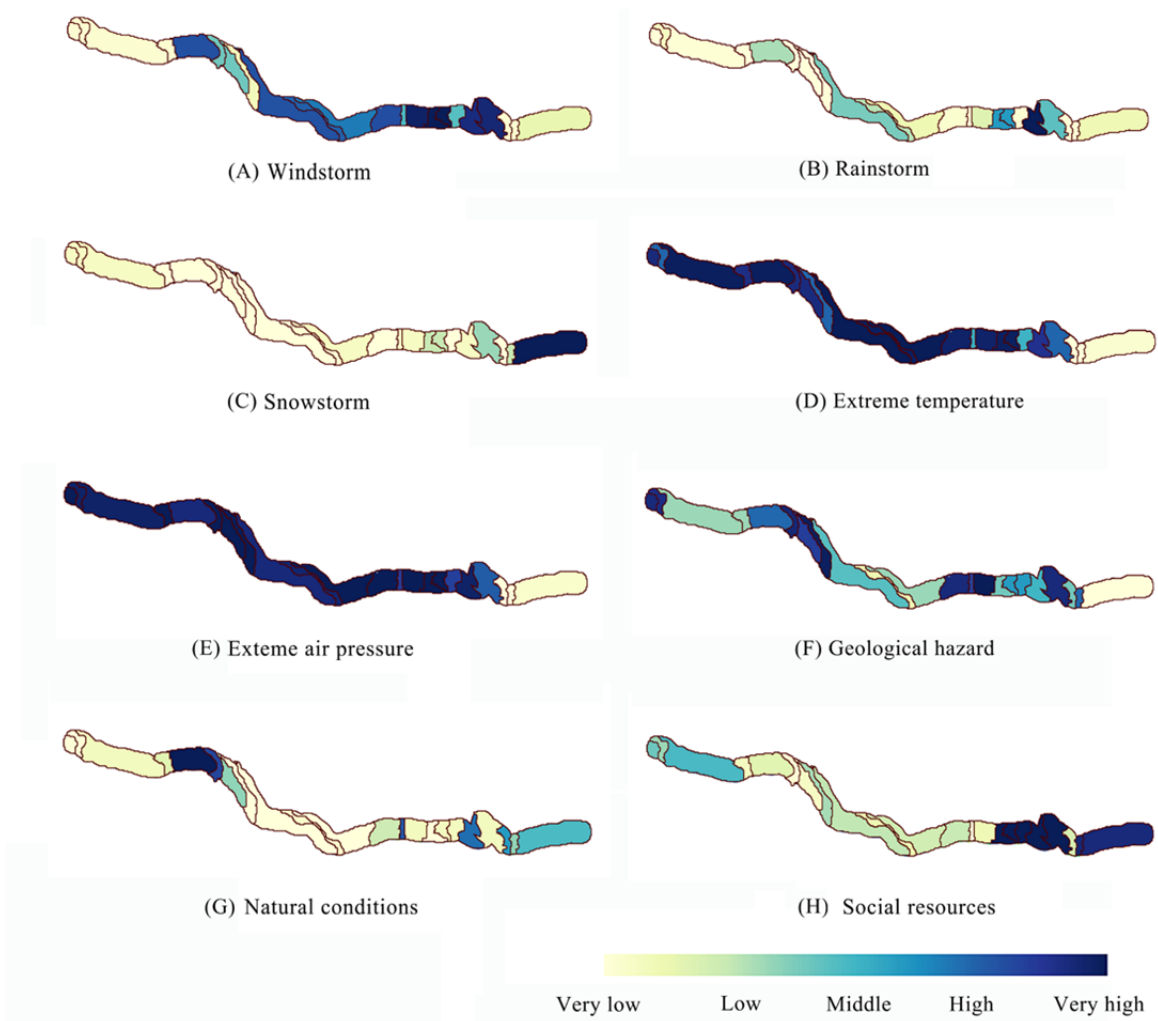Very low   Low   Middle   High   Very high

Fig. 5 Thermodynamic chart of scores for eight ecological vulnerability judgment indicators in 22 subzones.
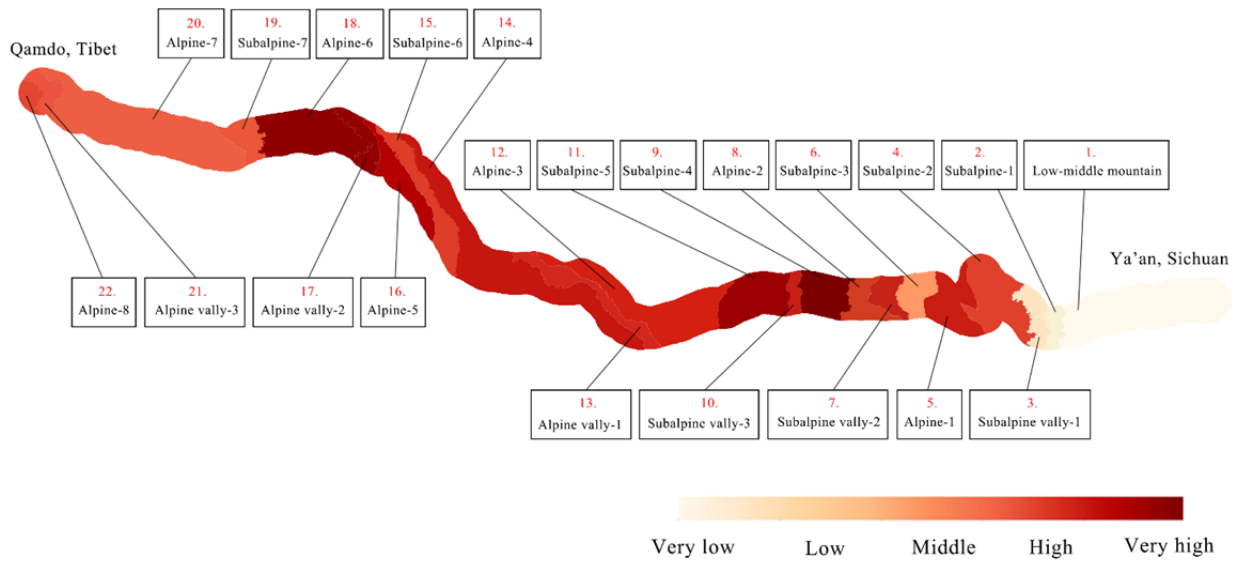

Fig. 6 Diagram of vulnerability assessment of the Ya'an-Qamdo section.

The classification matrix obtained from the clustering results is as follows.

$$C = \begin{bmatrix} 2 & 0 & 0 & 0 & 0 \\ 1 & 0 & 0 & 0 & 0 \\ 0 & 5 & 1 & 9 & 0 \\ 0 & 0 & 1 & 0 & 1 \\ 0 & 0 & 0 & 0 & 3 \end{bmatrix}$$

Then the separation and aggregation were calculated, and the results were $g = 122$, $d = 4$, $g' = 132$, $d' = 5$.

Therefore, $\eta = 0.74$ is relatively close to 1. The higher the similarity of A and B, the more rational the scoring of the eight indicators is.

5. 2 Validation of indicator weights

A cluster analysis of the eight indicators of the 22 subzones was carried out. Based on fuzzy matter-element analysis, the correlation coefficient value corresponding to each indicator of the 5 clustering centers was calculated so that the compound fuzzy matter-element is obtained as

$$L = \begin{bmatrix} 0 & 0.06 & 0.62 & 0.82 & 1 \\ 1 & 0 & 0.18 & 0.01 & 0.6 \\ 0.03 & 0.005 & 0 & 0.26 & 1 \\ 0 & 0.89 & 0.53 & 1 & 0.93 \\ 0 & 1 & 0.84 & 0.99 & 0.95 \\ 0 & 1 & 0.94 & 0.81 & 0.69 \\ 1 & 0 & 0.93 & 0.64 & 0.43 \\ 0.36 & 0.8 & 0.59 & 1 & 0 \end{bmatrix}$$

From the formula for R_w, we obtained:

$$R_w = [0.11, 0.08, 0.08, 0.15, 0.16, 0.18, 0.11, 0.13]$$

The values of R_w and L are then substituted by the correlation equation $R_k = R_w \cdot L$, which gives:

$$R_k = [0.32, 0.23, 0.60, 0.70, 0.65]$$

The vulnerability rating of the five clustering centers by the magnitude of the correlation is $\rho_2 < \rho_1 < \rho_3 < \rho_5 < \rho_4$, which is extended to the vulnerability rating of the 22 subzones:

$$Q = (2,3,1,21,15,20,19,22,6,10,4,5,8,7,14,16,13,18,12,17,11,9)$$

The vulnerability rating of the 22 subzones obtained in section 4.2 is:

$$P = (1,2,3,6,20,21,19,22,4,15,8,13,12,5,7,10,14,16,11,17,18,9)$$

By calculating the cosine of the angle between the two vectors, we get cosθ=0.931, which is very close to 1. Therefore, the weights calculated by the fuzzy matter-element analysis method are more rational.

6 Conclusion and Suggestions

The ranking of the indicator weights shows that extreme climate, frequent earthquakes, and lack of social resources are the driving factors of ecological vulnerability on the Ya'an-Qamdo section along the southern route of the Sichuan-Tibet transportation corridor. The vulnerability score and ranking shows that subzone 9 is the most vulnerable and subzone 1 is the least vulnerable. With diverse vegetation types and an ecosystem that is resistant to external disturbance, subzones 1 and 2, both located in the low- to mid-land warm and humid forest zone, covering Tianquan County, Dayuxi Township, and the main urban area of Ya'an City, Sichuan Province, are sthe least vulnerable. Subzone 9, located in the subalpine cold and humid forest and scrubland zone, covers Kangding City and Yajiang County, Ganzi Prefecture, Sichuan Province, where a large number of ethnic minorities live. Due to its large topographic relief, various natural hazards, and underdeveloped economy, subzone 9 lacks the ability to effectively resist and recover from external disturbances, making it very vulnerable. The results of the vulnerability ranking show that forest areas and gently sloping areas are less vulnerable.

This paper evaluated original data collected for each judgment indicator, used the fuzzy matter-element analysis method to rank the degree of ecological vulnerability, and verified the rationality of the evaluation model and assignment. Although some of the ranking results were a little different from what was expected, the overall results are consistent with professional empirical perceptions and are in line with common sense. Therefore, the research findings provide significant theoretical and data support for the ecological protection of the Sichuan-Tibet transportation corridor. Suggestions for follow-up studies are as follows: (1) There is still room for adjusting and improving the parameters and the verification method of the mathematical model. (2) Since the ecological vulnerability of Ya'an-Qamdo section involves other influencing factors, research methods from new perspectives need to be supplemented for cross-validation and improvement. Suggestions for planning and construction projects are as follows: (1) More attention should be paid to the dynamic patterns of local ecological vulnerability characteristics in regular forestry and natural resource management through leveraging scientific

methods. (2) The principle of avoidance in the permanent site selection of planning and construction projects is the priority in making ecological protection strategies. For example, we should avoid the most vulnerable subzones 9, 18, and 17 in surface engineering during the planning and construction, especially of permanent roads and large-scale land extraction and disposal sites. To reduce serious ecological damage that may hardly be recovered, we should analyze the key influencing factors of ecological restoration and then determine the restoration mode and measures for each subzone. (3) Scientific and technological research and field trial studies on solutions to ecological restoration and technology integration should be advanced actively in highly vulnerable subzones.

Acknowledgments

Open Access

References

Abson DJ, Dougill AJ, Stringer LC (2012) Using principal component analysis for information-rich socio-ecological vulnerability mapping in Southern Africa. Appl Geogr 35(1-2): 515-524.
https://doi.org/10.1016/j.apgeog.2012.08.004

Bao F, Qiu J (2021) Ecological vulnerability evaluation model of Sichuan-Tibet Railway based on fuzzy matter-element analysis. IOP Conference Series: Earth and Environmental Science.
https://doi.org/10.1088/1755-1315/760/1/012029

Chen J, Yang XJ, Yin S, et al. (2018) The vulnerability evolution and simulation of social-ecological systems in a semi-arid area: A case study of Yulin City, China. J Geogr Sci 28(2): 152-174.
https://doi.org/10.1007/s11442-018-1465-1

Chen Y, Xiong K, Ren X, et al. (2022) An overview of ecological vulnerability: a bibliometric analysis based on the Web of Science database. Environ Sci Pollut Res 29:12984-12996.
https://doi.org/10.1007/s11356-021-17995-1

Dagnino A, Sforzini S, Dondero F, et al. (2008) A "weight-of-evidence" approach for the integration of environmental "triad" data to assess ecological risk and biological vulnerability. Integr Environ Assess Manag 4(3): 314-326.
https://doi.org/10.1897/ieam_2007-067.1

Forootan E (2022) Erosion susceptibility assessment using fuzzy logic and multi-influencing factors combination approach. Arab J Geosci 15: 444.
https://doi.org/10.1007/s12517-022-09598-y

Frazier TG, Thompson CM, Dezzani RJ (2014) A framework for the development of the SERV model: A spatially explicit resilience-vulnerability model. Appl Geogr 51:158-172.
https://doi.org/10.1016/j.apgeog.2014.04.004

Gao JB, Hou WJ, Zhao DS, et al. (2016) Comprehensive assessment of natural ecosystem vulnerability in Tibetan

Plateau based on satellite-derived datasets. Sci Geol Sin 36(4): 580-587. (In Chinese)
https://doi.org/10.13249/j.cnki.sgs.2016.04.012

Guo B, Jiang L (2017) Evaluation of freeze-thaw erosion in Qinghai-Tibet Plateau based on multi-source data. Bulletin of Soil and Water Conservation 37(4): 12-19. (In Chinese)
https://doi.org/10.13961/j.cnki.stbctb.2017.04.003

Huang X, Jin H, Bai H (2019) Vulnerability assessment of China's coastal cities based on DEA cross-efficiency model. Int J Disaster Risk Reduct 36(4): 101091.
https://doi.org/10.1016/j.ijdrr.2019.101091

Jie XF, Jiang GJ, Xiao C, et al. (2015) Evaluation of ecosystem health in western Tiaoxi river watershed based on matter element model. Acta Sci. Circumst. 35(04): 1250-1258. (In Chinese)
https://doi.org/10.13671/j.hjkxxb.2014.0907

Kan AK, Li GQ, Yang X, et al. (2018) Ecological vulnerability analysis of Tibetan towns with tourism-based economy: A case study of the Bayi District. J Mt Sci 15(5): 1101-1114.
https://doi.org/10.1007/s11629-017-4789-x

Lai ZM (1996) Impact of climate variation on the runoff of large rivers in the Tibetan Plateau. J Glaciol Geocryol 18(z1): 314-320. (In Chinese)
https://doi.org/DOI:CNKI:SUN:BCDT.0.1996-S1-037

Li PX, Fan J (2014) Regional ecological vulnerability assessment of the Guangxi Xijiang River Economic Belt in Southwest China with VSD model. J Resour Ecol 5(2): 163-170.
http://doi.org/10.5814/j.issn.1674-764X.2014.02.009

Li Y, Tian Y, Li C (2011) Comparison study on ways of ecological vulnerability assessment – A case study in the Hengyang Basin. Procedia Environ Sci 10: 2067–2074.
https://doi.org/10.1016/j.proenv.2011.09.323

Li YN, Zhao XQ, Zhao L, et al. (2003) Analysis of vegetation succession and climate change in Haibei Alpine Marsh in the Qilian Mountains. J Glaciol Geocryol 25(3): 243-249. (In Chinese)
https://doi.org/10.3969/j.issn.1000-0240.2003.03.001

Luo L, Yan CG, Peng GZ (2005) Discussion on establishing a climatic and ecological monitoring system on the Eastern Qinghai-Tibetan Plateau. For Resour Manag 10(5): 66-76. (In Chinese)
https://doi.org/10.3969/j.issn.1002-6622.2005.05.015

Ma ZZ, Zhang MJ, Wang SJ, et al. (2019) Characteristics and differences of temperature rise between the Qinghai-Tibetan plateau region and northwest arid region of China during 1960-2015. Plateau Meteoro 38(1): 42-54. (In Chinese)
https://doi.org/10.7522/j.issn.1000-0534.2018.00074

Men BH, Liu HY (2018) Water resource system vulnerability assessment of the Heihe river basin based on pressure-state-response (psr) model under the changing environment. Water Sci Technol Water Supply 18(6): 1956-1967.
https://doi.org/10.2166/ws.2018.017

Ni CC, Li GP, Xiong XZ (2013) Validation of the applicability of AIRS data in Sichuan-Tibet Region of China. J Mt Sci 31(6): 656-663. (In Chinese)
https://doi.org/10.3969/j.issn.1008-2786.2013.06.003

Polsky C, Neff R, Yarnal B (2007) Building comparable global change vulnerability assessments: The vulnerability scoping diagram. Glob Environ Change 17(3-4): 472-485.
https://doi.org/10.1016/j.gloenvcha.2007.01.005

Qiao S (2013) Sun Yat-sen and his vision for the construction of the Sichuan-Tibet Railway. Fujian Tribune (The Humanities & Social Sciences Monthly) 05: 92-97. (In Chinese)
https://doi.org/DOI:CNKI:SUN:FJLW.0.2013-05-013

Song JY, Chung ES (2016) Robustness, Uncertainty and sensitivity analyses of the TOPSIS method for quantitative climate change vulnerability: a case study of flood damage. Water Resour Manag 30: 4751-4771.
https://doi.org/10.1007/s11269-016-1451-2

Song Z, Zhang GZ, Jiang LW, et al. (2016) Analysis of the characteristics of major geological disasters and geological alignment of Sichuan-Tibet Railway. Railw Stand Des 60(1): 14-19. (In Chinese)
https://doi.org/10.13238/j.issn.1004-2954.2016.01.003

Suter G, Nichols J, Lavoie E, et al. (2020) Systematic review and weight of evidence are integral to ecological and human health assessments: They need an integrated framework. Integr Environ Assess Manag 16(5): 718-728.
https://doi.org/10.1002/ieam.4271

Wang SY, Zhao MM, Yan J, et al. (2021) Evaluation on the importance of ecological protection in Changdu section of the Sichuan-Tibet Railway. Geosci 35(1): 234-243. (In Chinese)
https://doi.org/10.19657/j.geoscience.1000-8527.2021.006

Wang Y, Ran W, Wu L, et al. (2019) Assessment of river water quality based on an improved fuzzy matter-element model. Int J Environ Res Public Health 16(15): 2793.
https://doi.org/10.3390/ijerph16152793

Wei J, Guo YM, Sun L, et al. (2015) Evaluation of ecological environment vulnerability for Sanjiangyuan Area. Chin J Ecol 34(7): 1968-1975.(In Chinese)
https://doi.org/10.1017/S096402820426058X

Xia XS, Zhu XF, Li YC, et al. (2016) Evaluation for vulnerability of agroecological environment in Three Gorges Reservoir Area (Chongqing section) based on AHP-PCA entropy combination weight mode. J South Agric 47(4): 548-556. (In Chinese) .
https://doi.org/10.3969/j:issn.2095-1191.2016.04.548

Xu SG, Zuo YF, Zhang M (2021) Evaluation of tourism ecological security and diagnosis of obstacle factors in China based on fuzzy object element model. Sci Geol Sin 41(01): 33-43. (In Chinese)
https://doi.org/10.13249/j.cnki.sgs.2021.01.004

Xu YH (1991) Climate of Southwest China. China Meteorological Press, Beijing. (In Chinese)

Yang WC, Xu K, Lian JJ, et al. (2018) Integrated flood vulnerability assessment approach based on TOPSIS and Shannon entropy methods. Ecol Indic 89: 269-280.
https://doi.org/10.1016/j.ecolind.2018.02.015

Zhang C, Liu X (2013) A hybrid ANP-DEA approach for vulnerability assessment in water supply system. Proceedings of the Institute of Industrial Engineers Asian Conference. pp 1395-1403.
https://doi.org/10.1007/978-981-4451-98-7_164

Zhang H, Shen WS, Jiang LS, et al. (2004) Approach of evaluation on landscape protection along the Qinghai-Tibet Railway. Acta Ecol Sin 24(3): 574-582. (In Chinese)
https://doi.org/10.3321/j.issn:1000-0933.2004.03.027

Zhong XH, Liu SZ (2014) Research on the mountain classification in China. Mt Res 32(2):129-140. (In Chinese)
https://doi.org/10.16089/j.cnki.1008-2786.2014.02.006

Zhong XH, Liu SZ, Wang XD, et al. (2010) Research of ecological security on the Tibet Plateau. J Mt Sci 28(1): 1-10. (In Chinese)
https://doi.org/CNKI:SUN:SDYA.0.2010-01-003

Zou TH, Chang YX, Chen P, et al. (2021) Spatial-temporal variations of ecological vulnerability in Jilin Province (China), 2000 to 2018. Ecol Indic 133: 108429.
https://doi.org/10.1016/j.ecolind.2021.108429

Zou XH, Liu FG, Zhang YL, et al. (2013) County scale-based risk analysis of flood hazard in Qinghai-Tibet plateau. J Nat Disasters 22(5): 181-188. (In Chinese)
https://doi.org/CNKI:SUN:ZRZH.0.2013-05-024